International Conference on Lightning Protection
33rd International Conference on Lightning Protection
25 - 30 September 2016
Estoril, Portugal

A new class of electric discharges in clouds of negatively charged water droplets

Alexander Kostinskiy
National Research University Higher School of Economics
Moscow, Russia
kostinsky@gmail.com

Vladimir Syssoev, Mikhail Andreev, Dmitry Sukharevsky, Marat Bulatov
High-Voltage Research Center of the Zababakhin All-Russian Scientific Research Institute of Technical Physics
Istra, Moscow region, Russia
syssoev467@mail.ru

Evgeny Mareev, Nikolay Bogatov
Institute of Applied Physics, Russian Academy of Sciences
Nizhny Novgorod, Russia
mareev@appl.sci-nnov.ru

Vladimir Rakov
Department of Electrical and Computer Engineering
University of Florida,
Gainesville, USA
rakov@ece.ufl.edu

***Abstract* — We have observed unusual plasma formations (UPFs) in artificial clouds of charged water droplets using a high-speed infrared camera operating in conjunction with a high-speed visible-range camera. Inferred plasma parameters were close to those of long-spark leaders observed in the same experiments, while the channel morphology was distinctly different from that of leaders, so that UPFs can be viewed as a new type of in-cloud discharge. These formations can occur in the absence of spark leaders and appear to be manifestations of collective processes building, essentially from scratch, a complex hierarchical network of interacting channels at different stages of development (some of which are hot and live for milliseconds). We believe that the phenomenon should commonly occur in thunderclouds and might give insights on the missing link in the still poorly understood lightning initiation process.**

charged water droplets, electric discharges, long-spark leaders, streamers, lightning, high-speed infrared camera, unusual plasma formations (UPFs)

I. INTRODUCTION

Lightning is one of the most spectacular natural phenomena on Earth. However, in spite of a long history of lightning research ([1,2,3] and references therein), several fundamental problems concerning lightning physics unsolved. One of them is the mystery of lightning initiation in thunderclouds (the various lightning initiation theories are discussed, among others, [4,5,6]).

In this study, we used (a) artificial clouds of negatively charged water droplets with an average radius of 0.3–0.5 μm and (b) an infrared (IR) camera sensitive in the wavelength range of 2.7–5.5 μm to "see" what happens inside the cloud. We are not aware of any previous IR observations of electric discharges. Our cloud (10–15 m^3 in size), when negatively charged, is capable of drawing long sparks from nearby grounded objects [7] and, hence, can be viewed as a model of some natural charged aerosol systems. Our unique combination of cloud parameters (relatively small droplet size) and relatively long recorded wavelengths allowed us to observe a new class of in-cloud plasma formations, both in the presence and in the absence of sparks between the cloud and nearby grounded sphere. In our experiments, typically the best images of these unusual plasma formations are obtained when a spark is formed nearby. For this reason, most of the presented images correspond to this latter kind of the phenomenon. However, an example of unusual plasma formation (UPF) that occurred in the absence of spark leader is also given (see section II.C). The experimental setup is described in [8, 11]).

II. RESULTS

A. Two-Frame Infrared Record of Upward Positive Leader and Unusual Plasma Formation, Both Inside the Cloud [9]

Fig. 1 shows a still photograph (visible range, 3 s exposure) of a negatively charged cloud and four positive sparks, about 0.5–1 m in length. The average time interval between the four sparks was about 0.5–1 s. As expected, no luminous formations inside the cloud are seen in this visible-range image. Note that while the sparks in Fig. 1 are seen outside the cloud, most of the other images presented in this paper show discharge processes inside the cloud.

Fig. 2a and 2b show two consecutive frames taken by the IR camera viewing the upper part of cloud (the lower frame boundary was about 70 cm above the grounded plane). All the discharge processes seen in these frames were hidden inside the cloud and, hence, were not imaged in the visible range (only flashes of scattered light were observed). Each frame

had 6.7 ms exposure and 2ms dead time, so that the two images could be separated in time by 2 to 15.4 ms. It follows that most of the discharge processes recorded in the two frames were visible in IR for at least 2 ms. The processes seen

Fig. 1. Still picture (visible range; 3s exposure) of negatively charged cloud and four upward positive discharges, about 0.5–1 m in length.

in the IR images include (1) the upper, in-cloud part of the upward positive leader from the grounded sphere, whose

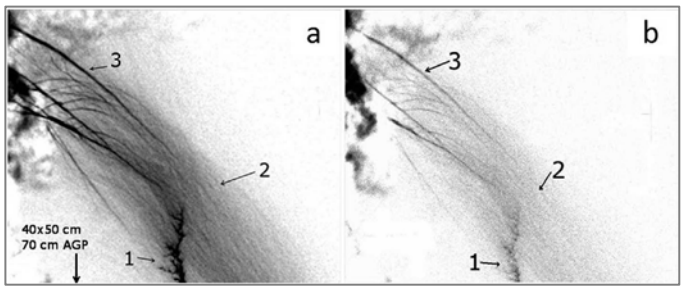

Fig. 2. Two consecutive infrared images (negatives) obtained with 6.7 ms exposure and separated by 2ms that show various discharge processes inside the cloud. Only flashes of scattered light, as opposed to distinct channels, were observed during this event in the visible range. 1: upper part of the upward positive leader (its lower part, developing in clear air, is outside the field of view of the IR camera), 2: streamer zone, 3: unusual plasma formation (UPF). AGP stands for "above the grounded plane."

lower part, developing in clear air, was outside the field of view of the IR camera; (2) a large streamer zone, crossing each frame from the lower right to the upper left corner (presumably positive corona from the upward positive leader channel, including its branches that are outside the camera field of view); and (3) unusual plasma formation (UPF) that is the focus of this paper. Both the imaged part of upward positive leader and the UPF appear to be inside or in the immediate vicinity of the streamer zone. The upward positive leader current had a peak of 5 A, lasted 35 μs, and transferred 15 μC of charge. No return-stroke-type process was observed. This UPF was formed as early as within 1.4 μs of the initial corona burst from the grounded sphere.

It is clear from Fig. 2 that the UPF is very different from either the upward positive leader or the streamer zone. Its brighter parts are much (an order of magnitude) brighter than streamers. Further, in Fig. 2a, the intensity of the IR radiation coming from some elements of UPF is similar to that coming from the hot upward-leader channel (this was determined both visually and quantitatively, using image analysis software). On the other hand, UPF morphology (a complex network of channels pervading a relatively large cloud region) does not resemble that of leader (main channel with branches indicating its direction of propagation and streamer zones at its extremities). In Fig. 2b, the UPF radiates even stronger than the decaying upward leader channel.

The IR images of UPF shown in Fig. 2a and 2b are typical in the presence of upward positive leader from the grounded sphere entering a negatively charged cloud. More than 100 of such events have been recorded to date.

B. UPF Located Below the Upper Part of the Upward Positive Leader Channel (Inside the Cloud)

Shown in Fig. 3 is an example of "nontypical" UPF that is oriented along the leader channel and located well below its upper part. Both are completely inside the cloud. The bright part of the UPF is 3–4 cm long and is accompanied by positive streamers developing predominantly upward, toward the negatively charged cloud and negative streamers interacting with the streamer zones of the lower branches of the upward positive leader. We also observed two well-defined and well-separated UPFs (each being similar to the one shown in Fig.3) that interacted with each other via their streamer zones. The UPF shown in Fig.3 appears to be qualitatively similar to the space stem/leader [10] involved in formation of negative-leader steps in long sparks and lightning, although it occurred in a very different context.

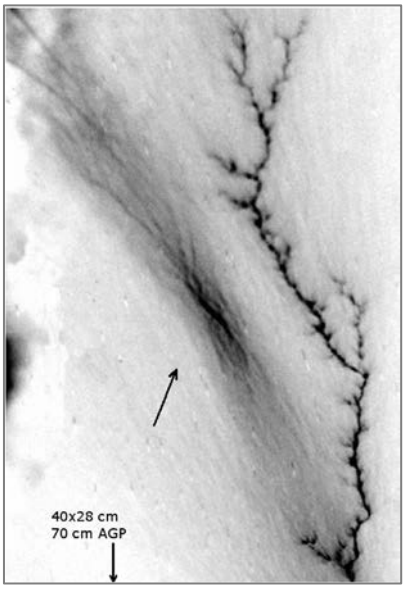

Fig. 3. Infrared image (negative) obtained with 6.7 ms exposure that shows the upper part of the upward positive (right) leader and (left) UPF, both inside the cloud; the slanted arrow points to the brightest part of UPF. The two appear to be distinct discharge processes which interact, via their streamer zones, in the lower part of the image. AGP stands for above the grounded plane.

C. UPF Occurring Without an Upward Positive Leader [9]

We observed that UPFs can take different forms and occur in different contexts, essentially anywhere in the cloud and in its immediate vicinity, with or without a spark discharge. An example of UPF without a spark is shown in Fig.4. Seen in Fig.4a is IR image of UPF recorded inside the cloud (to the right from its densest central part) in the absence of upward positive leader. Fig.4b is same as Fig.4a, but additionally showing a sketch of UPF superimposed on the image, in order to improve UPF visualization. It is not clear if the downward extending branches of UPF reach the grounded plane or not. Note the cellular structure of the UPF channel network, which is not observed in leaders. Similar structures can be also found in Fig. 2, 3, 5b, and 5c, but it is easier to locate in Fig.4 due to the relatively simple morphology of UPF it shows. Small solid circles in Fig.4b schematically show positions of increased brightness, possibly corresponding to space stems facilitating the formation of the cellular network structure of UPF.

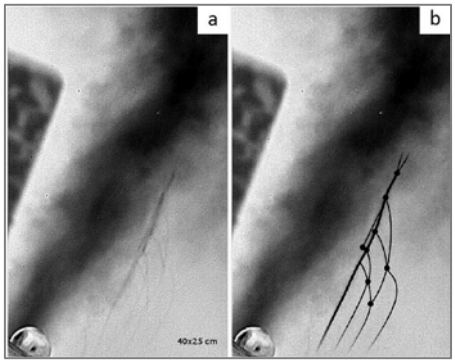

Fig. 4. (a) IR image of UPF recorded inside the cloud (to the right fromits densest central part) as a separate phenomenon; that is, without an upward positive leader. (b) Same as Figure 4a but additionally showing a sketch of UPF superimposed on the image in order to improve UPF visualization. It is not clear if the downward extending branches of UPF reach the grounded plane or not. Note the cellular structure of the UPF channel network, which is not observed in leaders

D. IR Probing of the Cloud and its Immediate Vicinity in Search for UPFs

Here we present results of IR probing of the cloud and its immediate vicinity by systematically changing the field of view of the IR camera, starting with the grounded sphere (from which the upward positive leader usually originates) and moving, in steps, up and to the left (toward the denser central part of the cloud). Representative images from this "scanning" are shown in Fig.5a–5d. In Fig.5a (the lowest and rightmost field of view), one can see only the upward positive leader from the grounded sphere, extending beyond the upper edge of the camera field of view. No UPF is seen, although it was likely present at higher altitudes. Fig.5b shows the upper part of the upward positive leader (Fig.5b, bottom right) and UPF (Fig.5b, top left). The two appear to be

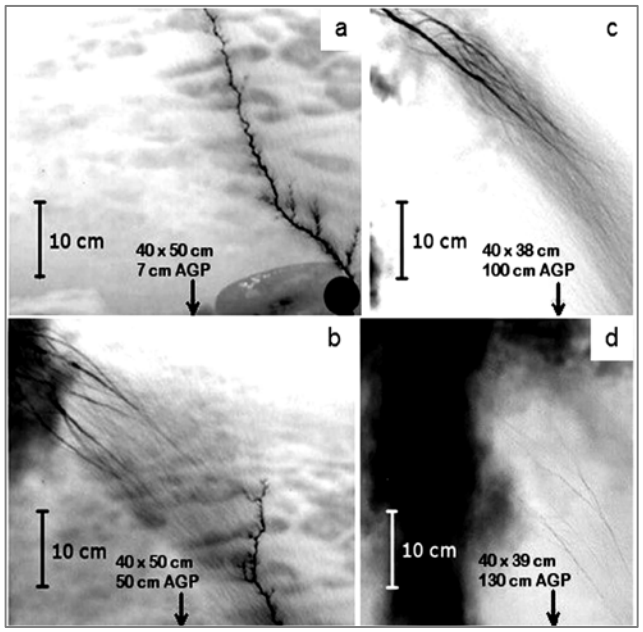

Fig. 5. Infrared images (negatives) obtained with 6.7 ms exposure that show the processes at different heights above the grounded plane (AGP) and different horizontal distances from the cloud axis: (a) The upward positive leader from the grounded sphere. No UPF is seen. (b) The upper part of the upward positive leader (bottom right) and UPF (top left), both inside the cloud. The two appear to be distinct discharge processes which interact, via their streamer zones. Relative to Figure 5a, the field of view of the IR camera was moved up and left (closer to the axis of the cloud). (c) The lower part of UPF (inside the cloud). The upward positive leader is outside the IR camera field of view, which was moved (relative to Figure 5b) further up and left. The upward positive leader and the UPF apparently interact (outside of the field of view) via their streamer zones. (d) Same as Figure 5c, but for the upper part of UPF near the central part of the cloud (see the dark formation on the left). Note that relatively faint UPF channels branch toward the axis of the cloud, but do not cross the axis This direction of branching is opposite to that seen in Figure 5c, suggesting that UPFs extend bidirectionally.

distinct discharge processes which interact, via their streamer zones. Similar to Fig. 2 and 3, the IR brightness of the most intense elements of the UPF is comparable to that of the leader channel (this was confirmed using image analysis software). The lower and upper parts of UPF can be seen in Fig.5c (note branching toward the upward positive leader) and 5d (note branching toward the densest central part of the cloud), respectively. Fig.5d corresponds to the highest and leftmost field of view of the camera in the scanning experiment.

Note that we could not image both the UPF and upward positive leader of the same event in their entirety (different fields of view were required for imaging different parts of the event), but the presented images of different parts of UPF-upward-positive-leader system are each representative of a large number of events generated at our installation.

Since the IR images presented here have never been reported before, it is interesting to check if the same

formations look different in the visible range. As noted above, observations of UPFs in the visible range are difficult, because the aerosol cloud droplet radius, typically about 0.5 μm, is close to the visible light wavelengths, so that the droplets effectively scatter visible light. The images, if obtained, are usually blurry and lack contrast. Usable visible-range images are rare. In supporting information section we have presented an example of simultaneous IR and rare visible-range images of the same UPF inside the cloud, where the latter image corresponds to a fragment of the former, but main features of the IR image are clearly identifiable in the visible-range one. It is likely that the visible-range imaging was made possible in this case by the proximity of UPF to the edge of the cloud, where the optical density of the cloud was relatively low.

E. Observation of UPFs in the visible range

Is it possible to record UPFs simultaneously in the visible and mid-IR ranges? Such measurements in the visible range are complicated by the fact that for the drop size of about 0.5 μm, visible light has a wavelength close to the size of the drops and is effectively scattered by them. The images, if obtained, are often vague and lack contrast. Despite this, we were able to simultaneously record UPFs in the visible and mid-IR ranges. Possibly, the UPFs were near the edge of the clouds and the optical density of the aerosol layer before a 4 Picos high-speed camera was low. A visible image of UPFs in Fig.6 was recorded by a 4 Picos camera aimed at the center of the aerosol clouds at a height of 80-120 cm above the plane where the ball is located. The camera was started from the current pulse coming from the ball through the shunt 400 ns after the initial flare of the corona. The exposure time was 1 μs. The picture is fuzzy but is clearly distinguishable since the UPFs are inside the cloud.

Fig. 6. The visible image taken by a 4 Picos camera aimed at the center of the aerosol cloud at a height of 80-120 cm above the plane where the ball is located. The camera was started by the current coming from the ball through the shunt 400 ns after the initial corona flare. Exposure time is 1 μs. The image is blurred since the UPFs are inside the cloud.

Fig.7 shows simultaneously an IR image of the same event as in Fig.6 with 8-ms exposure. In the upper left corner of Fig.7, for clarity, Fig. 6 shows a fragment depicting UPFs in the visible range. It is seen that the contours of the brightest UPFs are similar in the visible and near-IR images. The significant brightness superiority of one of the UPFs (the right-hand one) in the IR photographs can be attributed to its further development after the closing of the optical shutter of the 4 Picos camera.

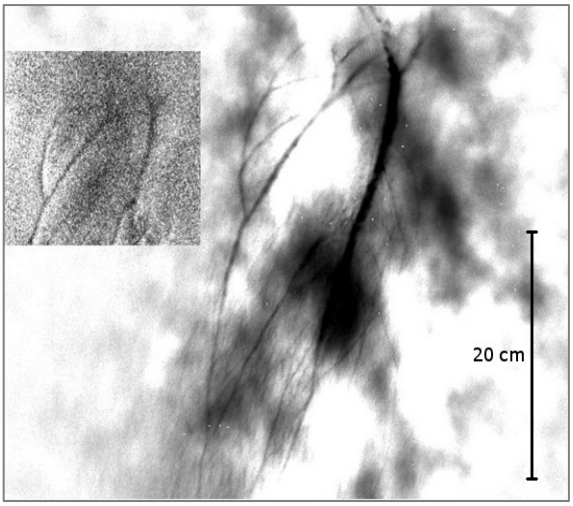

Fig. 7. Simultaneous IR image of the event recorded in Fig.6. Exposure time of the FLIR 7700M camera is 8 ms. Shown in the upper left corner is a fragment of Fig.6 depicting UPFs in the visible range. It can be seen that the contours of the brightest UPFs are similar in both images.

III. DISCUSSION

In order to check if the observed brightness of IR images of UPFs is indeed indicative of their high temperature, we examined the various sources of IR emission from electric discharges in air, including braking radiation and recombination radiation (in both cases continuous spectra), as well as radiation due to electron transitions between the higher electron levels of molecules and the radiation of vibrationally excited molecules (in both cases discrete spectra). Preliminary estimates based on the HITRAN 2012 molecular spectroscopic database [12] show that under the nonequilibrium discharge conditions, when the gas heating and excitation are insignificant, the main contribution to the emission in our IR camera sensitivity range (λ = 2.7–5.5 μm) comes from CO_2 molecules excited to several lower levels of the antisymmetric vibrational mode. These levels are in quasi-equilibrium with the vibrational levels of nitrogen molecules owing to the very efficient vibrational exchange between N_2 and CO_2 molecules whose corresponding energy levels are close to each other [13]. As a result, the intensity of recorded IR radiation is proportional to the degree of vibrational excitation of N_2. It is

known [14] that in nonequilibrium discharges in air the bulk of the energy input in gas goes to the vibrational excitation of N_2. Since the final gas temperature (after the vibrational-translational relaxation) is proportional to the energy input, and therefore to the degree of vibrational excitation of N_2 at the nonequilibrium stage, the intensity of recorded IR radiation can be viewed as a measure of the final gas heating in UPF, although this relationship is probably nonlinear. Based on our analysis, we conclude that the brightness of the IR images of UPFs reasonably represents the final gas temperature, which is reached as a result of the discharge process (leaving aside the issue of their size, since the brightness of optically thin objects is proportional to their spatial extent along the line of sight). A more detailed analysis of the air vibrational kinetics during the entire discharge process (including afterglow), needed for determination of quantitative relationship between the intensity of the IR radiation and the final gas temperature, is in progress.

We now discuss UPF morphology relative to that of leader. The UPF often involves a number of more or less parallel channels of relatively high brightness that are repeatedly interconnected by a great variety of fainter channels or branches (see Figures 2, 3, 5b, and 5c). As a result, the overall structure of UPF looks like a network of channels of irregularly varying brightness, which pervade a relatively large cloud region, in contrast with leaders which have a main channel with branches indicating its direction of propagation, more of less regularly varying brightness, and streamer zones at its extremities. Thus, the morphology of UPFs is distinctly different from that of leaders. Further, the secondary channels often appear to originate from and terminate on different points of the same trunk or originate from a common point in space and terminate on a neighboring channel, forming kind of loops or splits in the overall channel structure (see, in particular, the cellular structure of relatively simple UPF channel network in Fig.4a and 4b). The latter behavior (also seen with more effort in other, more complex UPFs) has never been observed in leaders. Nijdam et al. [15], using stereo photography, examined the so-called reconnection of positive streamers originated from the same metallic electrode in a short laboratory gap. They found that the reconnection was a result of attraction of a later streamer channel by an earlier streamer channel that has crossed the entire gap and possibly changed polarity. Clearly, this scenario is not applicable to our electrodeless discharges. Further, UPFs presented in this paper differ from streamers in that the former contain hot channel segments whose life time is of the order of milliseconds of more. Additionally, IR brightness of streamers in spark discharges differs substantially from that of leader, and a rather sharp boundary between the bright leader channel and the weakly glowing streamer zone is observed. In contrast, UPFs typically exhibit a more gradual change of luminosity along the channel (compare, for example, Fig.5a (leader) and 5c (UPF)). Based on the above, we conclude that UPF is a unique phenomenon, distinctly different from either leader or streamer.

How to interpret the observed UPF morphology? The basic reason for channel contraction in both streamers and leaders is the strong dependence of the electron-impact ionization rate on the so-called reduced electric field intensity, the latter being equal to the ratio of the actual electric field intensity and the air number density (E/N). This dependence provides the positive feedback leading to the fast decrease of the curvature of the ionized region (the channel tip radius) with the field growth in the case of avalanche-to-streamer transition and to the fast decrease of the air density with the temperature growth (due to the so-called thermalionizational instability) in the case of streamer-to-leader transition [3, pp. 27–88]. Different parts of UPFs develop in regions of different space-charge density, which can result in the inhomogeneous heating of plasma channel and triggering of the mechanism of thermal-ionizational instability at certain channel segments only (the process can even be aborted in the case of insufficient locally available charge). The described mechanism, taking into account the inhomogeneous charge distribution in the cloud, could explain a wide brightness spectrum of most of the observed UPFs and the variability of their structure. The nature of space-stem-like UPFs (see Fig.3) is less clear and requires further research.

We conclude with a brief discussion of some implications of our observations of UPFs in artificial clouds of charged water droplets for the improving of our understanding of lightning initiation process in thunderclouds. The lightning initiation mechanism remains a mystery, but researchers agree that it must involve the creation of a relatively large ionized region (“lightning seed”) in the cloud that is capable of locally enhancing the electric field at its extremities. Such field enhancement is likely to be the main process leading to the formation of a hot, self-propagating lightning leader channel. In our opinion, it is possible that UPFs are the key to understanding the lightning seed formation mechanism. Indeed, UPFs appear to be manifestations of collective processes building, essentially from scratch, a complex hierarchical system of interacting channels at different stages of development, some of which are hot and live for at least a few milliseconds. The basis for our speculation/prediction regarding UPF’s being possibly the missing link in the lightning initiation process is the fact that UPFs (1) occurred in charged cloud regions that did not previously host any detectable discharge activity and (2) contained hot channel segments in their overall network-like structure, while being distinctly different in their morphology from leaders. We believe that such formations can be an intermediate stage between virgin air (in the presence of water droplets) or initial low-conductivity streamer and a hot, self-propagating leader channel, provided that the hot segments of UPF can get polarized and grow within its overall channel network, thereby tapping energy from a relatively large cloud volume. In fact, it is possible that a UPF (a network of electrically floating plasma channels interacting with each other via positive and negative streamers) can serve to “metalize” a region of thundercloud, as described by Iudin et al. [16], thereby creating a “seed” needed for lightning initiation.

ACKNOWLEDGMENT

The authors thank Stanislav Davydenko, Nikolay Ilyin, Dmitry Iudin, Vladimir Klimenko, Leonid Makalsky, Yury Shlyugaev and Nikolay Slyunyaev for their useful discussions and are grateful to the Ministry of Education and Science of the Russian Federation for the financial support (project 14.B25.31.0023). The data reported in the paper are available upon request from the corresponding author A. Yu. Kostinskiy (kostinsky@gmail.com).

REFERENCES

[1] Rakov, V. A., and M. A. Uman, Lightning: Physics and Effects, Cambridge Univ. Press, Cambridge, 2003.

[2] Cooray, V. The Lightning Flash, 2nd ed.; The Institution of Engineering and Technology (IET): London, UK, 2014

[3] Bazelyan, E.M., Raizer, Y. P. Lightning Physics and Lightning Protection, 325 pp., IOP Publishing, Bristol, 2000.

[4] Rakov, V. A. Initiation of lightning in thunderclouds, Proc. SPIE, 5975, 362–373, doi:10.1117/12.675583, 2006.

[5] Gurevich, A. V., and A. N. Karashtin, Runaway breakdown and hydrometeors in lightning initiation, Phys. Rev. Lett., 110(18), 185005,

doi:10.1103/PhysRevLett.110.185005, 2013

[6] Sadighi, S., N. Liu, J. R. Dwyer, and H. K. Rassoul, Streamer formation and branching from model hydrometeors in subbreakdownconditions inside thunderclouds, J. Geophys. Res. Atmos., 120, 3660–3678, doi:10.1002/2014JD022724, 2015.

[7] Antsupov, K. V., I. P. Vereshchagin, M. A. Koshelev, L. M. Makalsky, and V. S. Syssoev, Discharges from cloud of charged aerosol, in Proc. 7th Int. Symp. on High Voltage Engineering, pp. 15–17, Tech. Univ. of Dresden, Dresden, Germany, 1991.

[8] Kostinskiy, A. Y., V. S. Syssoev, N. A. Bogatov, E. A. Mareev, M. G. Andreev, L. M. Makalsky, D. I. Sukharevsky, and V. A. Rakov, Infrared images of bidirectional leaders produced by the cloud of charged water droplets, J. Geophys. Res. Atmos., Volume 120, Issue 20, 27 October 2015, Pages 10,728–10,735, doi:10.1002/2015JD023827

[9] Kostinskiy,A.Y., V. S. Syssoev, N.A. Bogatov, E.A.Mareev, M. G.Andreev, L. M.Makalsky, D. I. Sukharevsky, and V. A. Rakov, Observations of a new class of electric discharges within artificial clouds of charged water droplets and its implication for lightning initiation within thunderclouds, Geophys. Res. Lett., 42, 16 October 2015 Pages 8165–8171. doi:10.1002/2015GL065620

[10] Les Renardières Group, Negative discharges in long air gaps at Les Renardières, 1978 results, Electra, 74, 67–216, 1981.

[11] A.Y.Kostinskiy, V.S.Syssoev, E.A.Mareev, V.A.Rakov, M.G.Andreev, N.A.Bogatov. L.M.Makal'sky, D.I.Sukharevsky, Electric discharges produced by clouds of charged water droplets in the presence of moving conducting object, Journal of Atmospheric and Solar-Terrestrial Physics 135 (2015) p.36–41, doi:10.1016/j.jastp.2015.10.00606

[12] Rothman, L. S., et al., The HITRAN2012 molecular spectroscopic database, J. Quant. Spectrosc. Radiat. Transfer, 130, 4–50, 2013. [Available athttp://hitran.iao.ru.]

[13] Cherrington, B., Gaseous Electronics and Gas Lasers, 226 pp., Pergamon, Oxford, 1979.

[14] Raizer, Y. P., Gas Discharge Physics, chap. 5.8, pp. 98–101, Springer, Berlin, 1991.

[15] Nijdam, S., C. G. C. Geurts, van Veldhuizen, E. M., and U. Ebert, Reconnection and merging of positive streamers in air, J. Phys. D Appl. Phys., 42, 045201, 2009, doi:10.1088/0022-3727/42/4/045201.

[16] Iudin, D. I., V. Y. Trakhtengerts, and M. Hayakawa, Fractal dynamics of electric discharges in a thundercloud, Phys. Rev. E, 68(1), 016601, 2003, doi:10.1103/PhysRevE.68.016601.